An Adaptive Data Processing Technique for Lidar-Assisted Control to Bridge the Gap between Lidar Systems and Wind Turbines

David Schlipf[1,2], Paul Fleming[2], Steffen Raach[1], Andrew Scholbrock[2], Florian Haizmann[1], Raghu Krishnamurthy[3], Matthieu Boquet[3], and Po Wen Cheng[1]

[1]Stuttgart Wind Energy (SWE) @ Institute of Aircraft Design, University of Stuttgart, Germany.
[2]National Renewable Energy Laboratory (NREL), Boulder, Colorado, USA.
[3]Avent Lidar Technology, Orsay, France.

Abstract

This paper presents first steps toward an adaptive lidar data processing technique crucial for lidar-assisted control in wind turbines. The prediction time and the quality of the wind preview from lidar measurements depend on several factors and are not constant. If the data processing is not continually adjusted, the benefit of lidar-assisted control cannot be fully exploited or can even result in harmful control action. An online analysis of the lidar and turbine data is necessary to continually reassess the prediction time and lidar data quality.

In this work, a structured process to develop an analysis tool for the prediction time and a new hardware setup for lidar-assisted control are presented. The tool consists of an online estimation of the rotor effective wind speed from lidar and turbine data and the implementation of an online cross-correlation to determine the time shift between both signals. Further, we present initial results from an ongoing campaign in which this system was employed for providing lidar preview for feedforward pitch control.

1 Introduction

For wind turbines, wind is the energy source as well as the main disturbance to the wind turbine control system. The control system has to balance competing control objectives: increasing the energy yield while reducing the structural loads. However, traditional feedback controllers are only able to react to the disturbance of the inflowing wind field after it has already impacted the turbine. With the recent development of lidar technology, the information about incoming disturbances can be made available ahead of time and used for feedforward control. A comprehensive overview of lidar-assisted control can be found in [1].

In an initial field testing on the two- and three-bladed Controls Advanced Research Turbines (CART2 and CART3 at the National Wind Technology Center in Boulder, Colorado), a collective pitch feedforward controller using lidar wind disturbance preview was able to reduce the rotor speed variation [2, 3]. However, this reduction cannot be directly converted into a reduction of the levelized cost of energy (LCOE). Thus, one of the long-term research challenges identified by the European Academy of Wind Energy is the transformation from scientific proof-of-concept to studies that provide a measurable benefit of lidar-assisted control [4]. A first study shows an LCOE reduction of 6.5% for large offshore wind turbines [5].

Lidars are only able to measure the wind speed along the line-of-sight (LOS) of the laser beam. Multiple LOS measurements can be put together to form a general wind field, with a longitudinal wind speed, as well as horizontal and vertical shear. Additionally, these wind speed measurements are taken upstream of the wind turbine, and as the wind travels toward the wind turbine, it will change due to the turbulence in the atmosphere. A coherence measurement between the lidar wind measurement and the rotor effective wind speed measured by the wind turbine helps to quantify the turbulent wind evolution. Higher and higher coherence values will lead to further and further improvements in the controller's ability to use the lidar preview information for feedforward control. An example of this is in [6], where simulation studies showed that improving the coherence will lead to improvements in feedforward control for load reductions.

Having a high coherence between the lidar measured wind speed and the rotor effective wind speed is quite challenging, as the coherence has to take into account the lidar measurement techniques as well as the turbine dynamics. From an industrial standpoint, lidars and wind turbines come from different manufacturers and have their own individual data acquisition systems. Additionally, due to the multi- and interdisciplinary character of the problem, there is a gap in knowledge: on the one hand, a thorough understanding of lidar measurement principles and limitations is mandatory for providing usable signals to the con-

trol system. On the other hand, detailed knowledge about wind turbine dynamics and controls are necessary to determine which signals can be used for preview control. These challenges make it hard for lidars and wind turbines to relate to one another in order to effectively enhance the turbine control system with lidar wind preview. Instead, a centralized system—developed by a joint project between industry and research institutions—which has access to real-time data from both the wind turbine and the lidar, would be better suited to close the gap between lidars and wind turbines.

A consortium of NREL, SWE, and the lidar manufacturer Avent Lidar Technology started to test advanced lidar-assisted control on the CART2 in January 2015. The same lidar-turbine combination has been used in an previous campaign [7]. A new adaptive data processing technique independent from lidar and turbine control software and hardware was developed during this campaign. The improved setup and the combination of lidar- and turbine-specific knowledge enables a comparison of the rotor-effective wind estimates from turbine and lidar data. With a cross-correlation calculated in real time, the lidar estimate can be aligned with the turbine's reaction via a graphical user interface (GUI). The feedforward control action can be applied to the turbine with the desired preview time, which improves the overall control performance.

This system was then used to provide a feedforward pitch update to the feedback controller, and a campaign to assess the improvement in performance from the baseline controller was performed. Initial results from this campaign are provided to show the value of the approach.

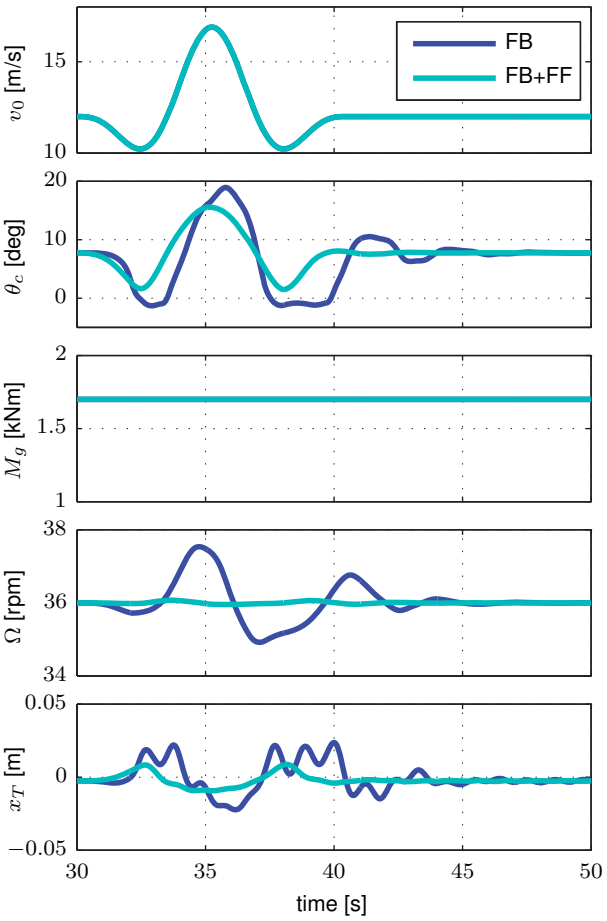

Figure 1: Reaction to an EOG at 12 m/s: Feedback only (dark blue) and with additional feedforward (light blue).

2 Approach

As discussed in the introduction, this paper presents a system for producing an accurate wind preview that can be used for maximally effective feedforward control of wind turbines.

In this section, we present the approach taken for designing this complete system, from the design of the feedforward controller that will apply the lidar signal, the development of the data processing that produces the signal, and the stages of refinement and implementation that would be expected in an industrial application.

2.1 Structured Code Development for Lidar-Assisted Control

The code development for lidar-assisted control is structured in five stages: feedforward controller development, data processing development, real-time environment development, hybrid simulations, and field testing.

1. *Feedforward Controller Development*: Assuming perfect wind preview, the feedforward controller is first designed and tested using the Simplified Low Order Wind turbine (SLOW) model [8] with only 2 degrees-of-freedom (rotor and tower motion). In this case, the simulation model is identical to the controller design model and the control performance should be as desired. Then, the same wind is used in simulations with an aeroelastic model (FAST [9]) to test the robustness of the controller against model uncertainties. Figure Figure 1 shows simulations with the FAST model for an extreme operating gust (EOG). The feedforward controller is able to reduce the impact of wind speed changes to the rotor speed following its design objective [10]. Figure 2 (left) shows a diagram of the SLOW model.

2. *Data Processing Development*: In the previous stage, the feedforward controller was designed to perform well assuming perfect wind preview. In this stage, we develop the data processing that will be used given realistic lidar measurement of the wind. Using the FAST model, we now simulate the turbine operating in a turbulent wind field, rather than a uniform flow, which can be easily represented by a single velocity. A lidar simulator [11] is used to scan the incoming wind field. The data is condensed to an estimate of

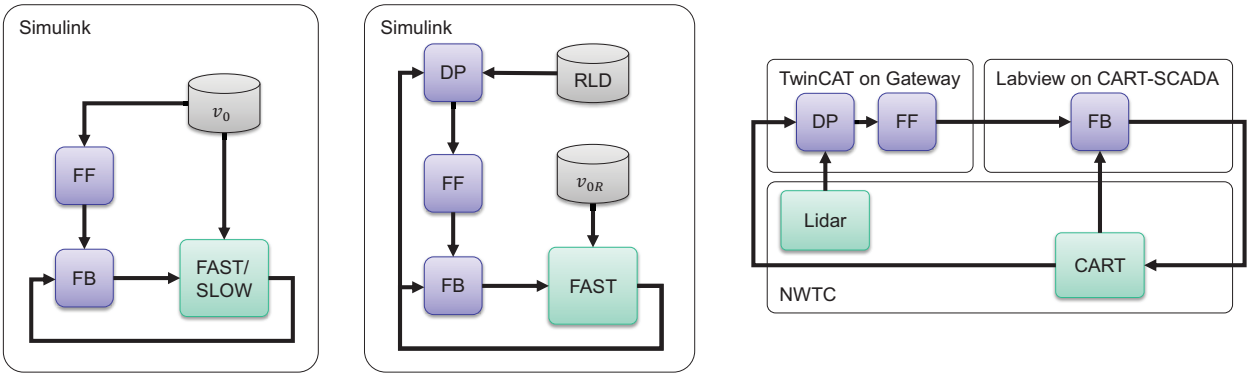

Figure 2: Code development. Stage 1 (left): Simulation within Simulink with perfect wind preview; the rotor-effective wind v_0 disturbs the turbine and the feedforward controller (FF) is designed to assist the feedback controller (FB). Stage 4 (center): Hybrid Simulations within Simulink; the rotor-effective wind speed from field test turbine data v_{0R} and simultaneously measured field test raw lidar data (RLD) are used to adjust the data processing (DP). Stage 5 (right): Field Testing; the DP and FF are compiled for TwinCAT on the Gateway and the FB for Labview on the CART-SCADA.

the rotor-effective wind speed, filtered, and transferred to the feedforward controller. The data processing can be evaluated by comparing the correlation between the lidar estimate and the real rotor-effective wind speed to a correlation model [12, 13]. Simulations are done over the full operation range to test the robustness of the controller against measurement uncertainties.

3. *Real-Time Environment Development*: The data processing system and the feedforward controller are compiled to be used within a real-time capable frame (TwinCAT) on a separate computer (referred in this work as "Gateway"). The same simulations from Stage 2 are done and thus allow a direct verification of the real-time environment.

4. *Hybrid Simulations*: Effects such as the wind evolution can be included [14] in simulations, but effects such as measurement errors and changing lidar data quality are difficult to simulate. Thus, the approach of the Hybrid Simulations [15] is used to adjust the lidar data processing and feedforward controller: The rotor-effective wind speed is extracted from real turbine data [16] and together with simultaneously measured lidar data used for simulations, as shown in Figure 2 (center).

5. *Field Testing*: Finally, following the above iterations, the Gateway is connected to the actual lidar and turbine controller, as shown in Figure 2 (right).

The approach has several advantages:

- The feedforward controller, the data processing, and the real-time environment are developed independently. Thus, the data processing can be combined with different feedforward controllers.

- Each stage has a defined goal. This helps to develop several controllers in parallel.

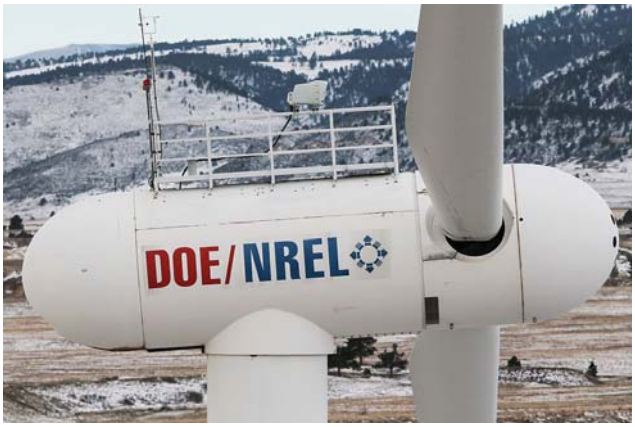

Figure 3: The Avent 5-Beam installed on the nacelle of the CART2 at the NWTC. (Photo Credit: Lee Jay Fingersh, NREL 33621)

- The code is developed in the control-engineer-friendly Simulink environment and is organized in one single library. Thus, adjustments can be directly transferred to other stages.

2.2 Hardware Setup for Lidar-Assisted Control

The CART2, located at the National Wind Technology Center (NWTC), is a 600-kW turbine heavily instrumented with sensors. A control system (CART-SCADA) was developed and implemented in Labview by NWTC engineers running at 400 Hz, containing a dynamic link library (DLL) compiled from the Simulink-based feedback controller.

The Avent 5-Beam pulsed system was installed on the nacelle of the CART2 (see Figure 3) and measures at 10 distances in front of the rotor. At each distance, five line-of-sight measurements are taken sequentially within 1.25 seconds and are transferred to the CART-SCADA via an Ethernet connection in real time.

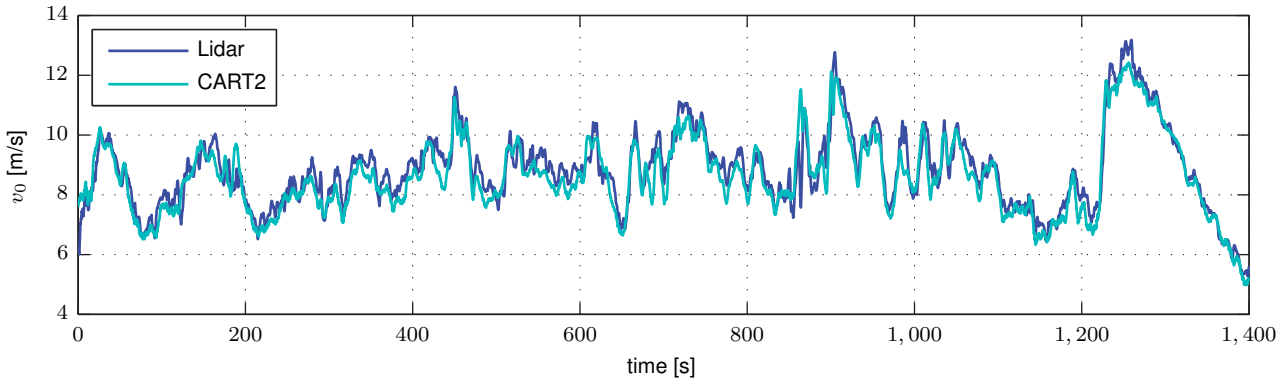

Figure 4: Rotor effective wind speed: from CART2 data (light blue) and lidar data (dark blue).

The data processing and feedforward controller are realized on the Gateway, which is a deterministic, real-time capable industrial PC and is connected to the CART-SCADA via an Ethernet connection. The lidar data is condensed into an estimate of the lidar-measured rotor-effective wind speed. Additionally, the Gateway receives turbine data, including rotor speed, blade pitch angle, and rotor shaft torque, to obtain the turbine-measured rotor-effective wind speed. The Gateway provides its feedforward update signals to the CART-SCADA, and the CART-SCADA can independently choose whether or not to use the signals in order to provide robust operation.

A separate computer connected to the Gateway visualizes the processed data and offers a way to directly interact with the Gateway via a GUI. Further, the feedforward control action (blade pitch, generator torque, desired rotor speed) are compared to measured data. Additionally, the software provides the possibility of adjusting parameters used for the online cross-correlation that will be described in the next section.

3 Results

3.1 Correlation Study

Similar to previous work, the rotor effective wind speed estimated from the raw lidar data and from the turbine reaction has been compared before the feedforward controller was applied. Figure 4 compares both signals in the time domain. Larger trends, such as the gust at the end of the period, are very well detected by the lidar.

This is confirmed by Figure 5, which compares both signals in the frequency domain: for small wavenumbers (large turbulent eddies) the coherence is close to one (1 means perfect correlation), and for larger wavenumbers (smaller turbulent eddies) the coherence γ^2_{RL} is going toward zero (0 means no correlation). The correlation is verified by the analytical model [12]. The longitudinal decay parameter for the wind evolution was set to 0.2 based on the detected value from [17].

The detected correlation is used to design an adaptive filter, which adjusts the cut-off-frequency depending on the mean wind speed. In future work, the adaptation needs to be extended to detect changes in the correlation and adjust the filter accordingly.

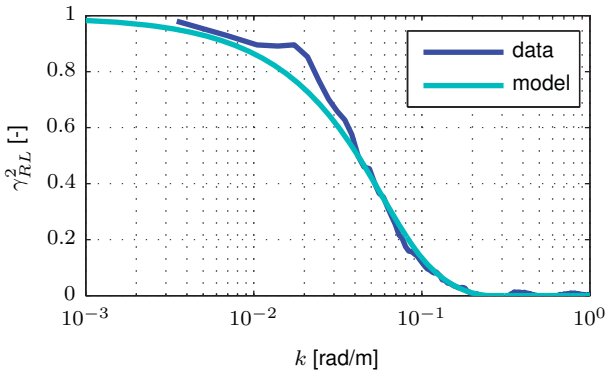

Figure 5: Coherence between the lidar and turbine estimate of the rotor-effective wind speed: From data of Figure 4 (dark blue) and from analytic correlation model (light blue).

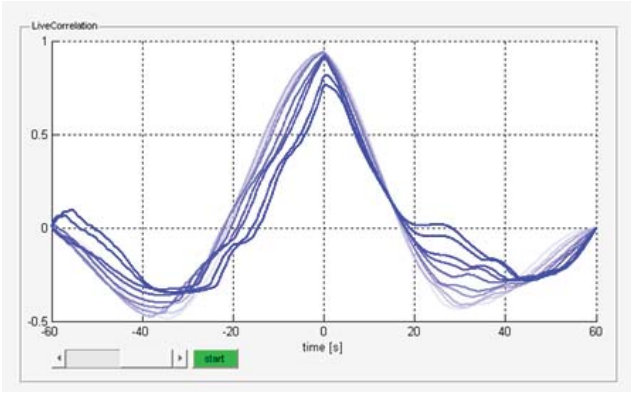

Figure 6: Cross-Correlation between the lidar and turbine estimate of the rotor-effective wind speed over the last 10 s: Newest (dark blue) and oldest (light blue) data.

3.2 Online Calculation of Cross-Correlation

The feedforward control inputs are calculated based on the lidar estimate of the rotor-effective wind speed and sent to the CART-SCADA with an adjustable preview time before the wind disturbance reaches the turbine. This timing is crucial and the lidar estimate needs to be aligned with the rotor-effective wind speed from the turbine data. The preview time of the lidar estimate is based on Taylor's Frozen Turbulence Hypothesis and calculated by dividing the measurement distance by the mean wind speed. Changes in the preview can be due to the changing impact of the induction zone or inaccuracies in Taylor's hypothesis or the measurement distance.

On the Gateway, the timing is evaluated online by calculating the cross-correlation between the rotor-effective wind speed from lidar and turbine data. The normalized cross-correlation gives a measure of the similarity of the estimation and the timing of the estimation. An example of the online cross-correlation over the last 10 seconds is given in Figure 6. The timing can be adjusted manually by shifting the lidar preview via the GUI, and the changes can be observed in real time. During the ongoing field testing, an offset of 1 second was identified and corrected.

3.3 Initial Results of Field Testing

Finally, a field-campaign was conducted in which the baseline feedback pitch controller was augmented by the lidar-preview feedforward pitch update. Because the lidar preview measurement was shown to have good coherence to turbine measurements and was robust over time, the feedback controller could be detuned to maximize the benefit of using lidar feedforward. Detuning the feedback controller allows the feedforward controller to handle the lower wind disturbance frequencies, up to the coherence limit, which should be the optimal combination.

The field test is set up so that the controller cycles between 5 minutes of running the normal baseline feedback controller and 5 minutes of combined a feedforward and detuned feedback controller as described above. By cycling in this way, the two controllers are tested in wind conditions that are as similar as possible.

Currently, field tests have been run intermittently over several months, across a range of seasons and atmospheric conditions. While still somewhat initial, the data is already demonstrating promising trends. To analyze the data, we process each 5-minute data file as follows. The first 30 seconds of each file are ignored, to allow the change in performance of transitioning from one controller to another to be established. The remaining time is divided in 45-second continuous chunks and processed. For each chunk, statistics such as mean and standard deviation are computed for all signals, and for signals related to fatigue, a damage equivalent load (DEL) is likewise computed.

We first consider the speed-regulation performance of the lidar-enhanced controller compared to the baseline. The collective pitch controller regulates the rotor speed to the rated setpoint. The first question to answer is how has our modification affected this performance.

Figure 7 compares the performance of speed regulation. Note that for the plots, the statistics computed from the 45-second chunks have been binned by wind speed, and for each wind speed and controller the mean value and standard error of the mean are computed. First, in Figure 7 (left), the standard deviation of the rotor speed is compared across the collected 45-second chunks of data. From this plot, it appears that the speed regulation performance has not been impacted, which is the desired result. Had lidar feedforward been ineffective, detuning the feedback controller would have significantly worsened and rotor speed variation would have increased. Figure 7 (right) plots the frequency of occurrence of each per-chunk maximum rotor speed. While the highest observed rotor speeds did occur with the lidar-enhanced controller, there is not much noticeable change in performance. Finally, Figure 8 (left) shows the pitch rate standard deviation, which indicates the amount of pitch activity. Here, it is clear the lidar-enhanced controller is achieving similar results in speed-control with significantly less pitch actuation when compared to the feedback-only controller. Because the feedback controller can only react after a wind event, it would normally need to pitch more aggressively than a controller that previews the upcoming wind event and can begin acting ahead of time.

Additionally, the standard deviation of the tower acceleration in Figure 8 (right) is reduced. We can now compare the controllers in terms of the fatigue loads by plotting the per-chunk DEL statistics. Because collective pitch is most tightly coupled to fatigue loads related to rotor thrust, we focus on those—specifically blade flap bending moment and tower fore-aft bending moment.

The comparison of flap bending is shown in Figure 9 (left). Although additional data collection in higher winds would greatly aid in drawing conclusions, a reduction in this load is evident in wind speeds above rated. Fore-aft tower bending, shown in Figure 9 (right), is significantly reduced by the experimental controller.

4 Conclusion and Outlook

In this work a solution is presented that allows the data processing and feedforward control to be independently calculated of the lidar system and the turbine controller. This setup allows robust operation of the wind turbine and intensive calculations on time scales different from the feedback control loop.

Further, the setup provides the possibility to determine not only the rotor-effective wind speed estimate

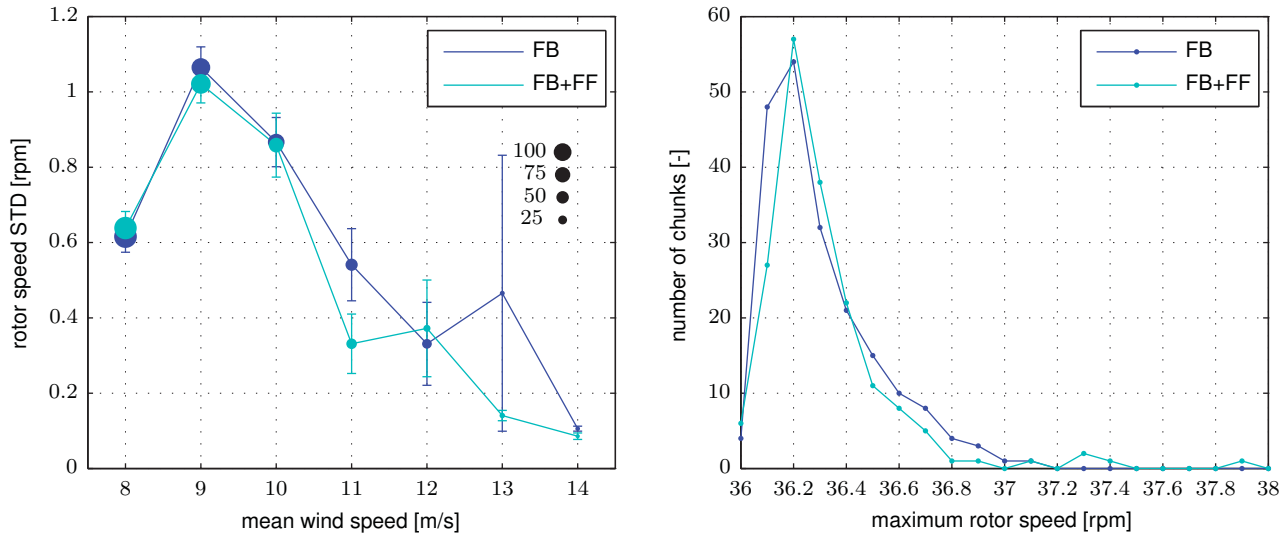

Figure 7: Comparing controller effects on rotor speed regulation. Left: standard deviation of rotor speed. The points are the mean value for each bin, while the error bars indicate the standard error of the mean. Right: frequency of occurrence of each per-chunk maximum rotor speed.

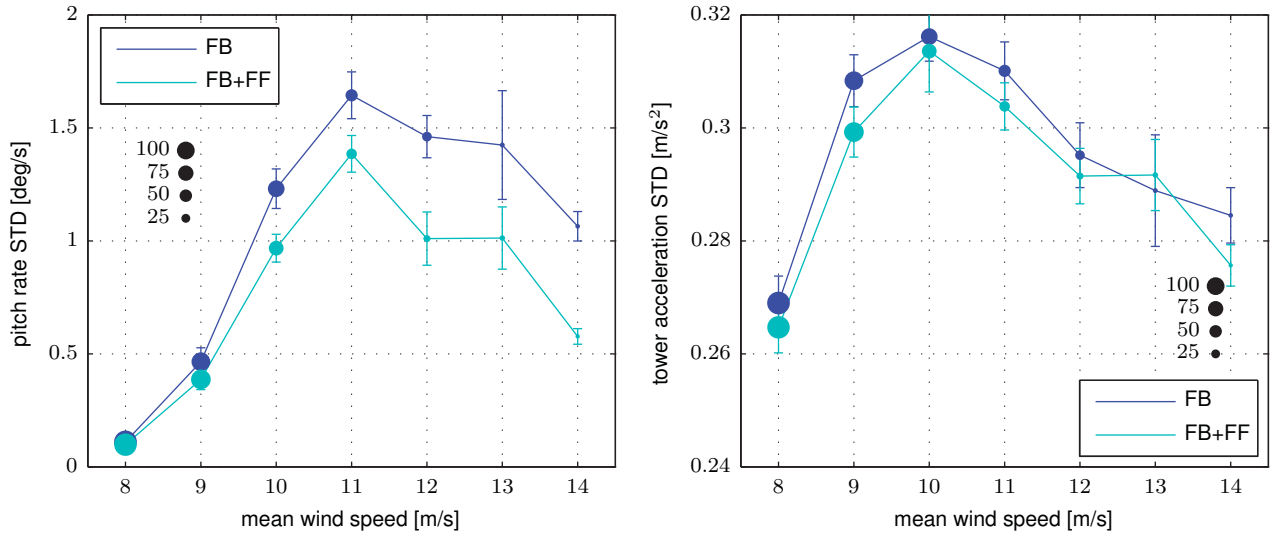

Figure 8: Comparing controller on standard deviation of pitch rate (left) and tower acceleration (right). The points are the mean value for each bin, while the error bars indicate the standard error of the mean.

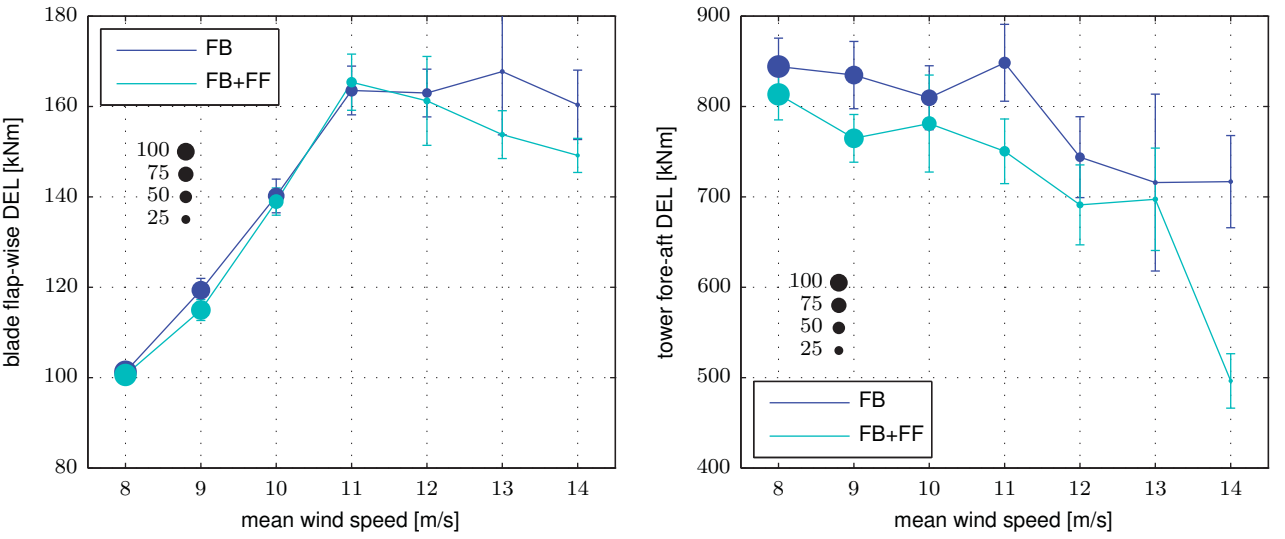

Figure 9: Comparing controller effects on loads. Blade flap-wise bending (left) and tower fore-aft bending (right). The points are the mean value for each bin, while the error bars indicate the standard error of the mean.

from the lidar data that is used for lidar-assisted control but also of the rotor-effective wind speed from the turbine data. Using both signals, an online cross-correlation is computed and visualized allowing an adjustment of the timing of the lidar-assisted control. This improves the performance of the feedforward controller.

Results of field testing a feedforward controller designed using the above approach indicate success in improving the performance over the baseline feedback controller, in terms of both reduced actuation usage and reduced fatigue loads.

In future work, the setup will be extended by an automated adjustment of the timing and filtering once the method has been proven to be robust. The Gateway will be used for advanced feedforward controllers such as the flatness-based approach [18] and Nonlinear Model Predictive Control [19, 20].

5 Acknowledgments

This work was supported by the U.S. Department of Energy under Contract No. DE-AC36-08GO28308 with the National Renewable Energy Laboratory. Funding provided by the DOE Office of Energy Efficiency and Renewable Energy, Wind and Water Power Technologies Office.

References

[1] E. Bossanyi, A. Kumar, and O. Hugues-Salas, "Wind turbine control applications of turbine-mounted lidar," *Journal of Physics: Conference Series*, vol. 555, no. 1, p. 012011, 2014.

[2] D. Schlipf, P. Fleming, F. Haizmann, A. Scholbrock, M. Hofsäß, A. Wright, and P. W. Cheng, "Field testing of feedforward collective pitch control on the CART2 using a nacelle-based lidar scanner," *Journal of Physics: Conference Series*, vol. 555, no. 1, p. 012090, 2014.

[3] A. Scholbrock, P. Fleming, L. Fingersh, A. Wright, D. Schlipf, F. Haizmann, and F. Belen, "Field testing LIDAR based feed-forward controls on the NREL controls advanced research turbine," in *Proceedings of the 51st AIAA Aerospace Sciences Meeting Including the New Horizons Forum and Aerospace Exposition*, Dallas, USA, 2013.

[4] European Academy of Wind Energy. Long-term research strategy. www.eawe.eu.

[5] D. Arora and C. Carcangiu, "Advanced controls for cost of energy reduction of floating offshore wind turbines," in *Presentation at the EWEA Offshore*, Copenhagen, Denmark, 2015.

[6] J. Laks, L. Y. Pao, A. Wright, N. Kelley, and B. Jonkman, "Blade pitch control with preview wind measurements," in *Proc. AIAA Aerospace Sciences Meeting*, Orlando, Florida, USA, January 2010.

[7] A. A. Kumar, E. A. Bossayni, A. K. Scholbrock, P. A. Fleming, M. Boquet, and R. Krishnamurthy, "Field testing of lidar assisted feedforward control algorithms for improved speed control and fatigue load reduction on a 600kw wind turbine," in *EWEA 2015 Conference Proceedings In Press*, Paris, France, November 2015.

[8] C. L. Bottasso, A. Croce, B. Savini, W. Sirchi, and L. Trainelli, "Aero-servo-elastic modelling and control of wind turbines using finite-element multibody procedures," *Multibody System Dynamics*, vol. 16, no. 3, pp. 291–308, 2006.

[9] J. Jonkman and M. L. Buhl, "FAST user's guide," NREL, Tech. Rep. EL-500-38230, August 2005.

[10] D. Schlipf, T. Fischer, C. E. Carcangiu, M. Rossetti, and E. Bossanyi, "Load analysis of look-ahead collective pitch control using LiDAR," in *Proceedings of the German Wind Energy Conference DEWEK*, Bremen, Germany, 2010.

[11] D. Schlipf, "Lidar-assisted control concepts for wind turbines," Ph.D. dissertation, University of Stuttgart, under review, 2015.

[12] D. Schlipf, J. Mann, and P. W. Cheng, "Model of the correlation between lidar systems and wind turbines for lidar assisted control," *Journal of Atmospheric and Oceanic Technology*, vol. 30, no. 10, pp. 2233–2240, 2013.

[13] E. Simley and L. Y. Pao, "Correlation between rotating LIDAR measurements and blade effective wind speed," in *Proceedings of the 51st AIAA Aerospace Sciences Meeting Including the New Horizons Forum and Aerospace Exposition*, Dallas, USA, 2013.

[14] E. Bossanyi, "Un-freezing the turbulence: improved wind field modelling for investigating lidar-assisted wind turbine control," in *Proceedings of the European Wind Energy Association annual event*, Copenhagen, Denmark, 2012.

[15] D. Schlipf, P. Fleming, S. Kapp, A. Scholbrock, F. Haizmann, F. Belen, A. Wright, and P. W. Cheng, "Direct speed control using lidar and turbine data," in *Proceedings of the American Control Conference*, Washington, DC, USA, 2013.

[16] E. van der Hooft and T. G. van Engelen, "Estimated wind speed feed forward control for wind turbine operation optimization," in *Proceedings of the European Wind Energy Conference*, London, UK, November 2004.

[17] D. Schlipf, F. Haizmann, N. Cosack, T. Siebers, and P. W. Cheng, "Detection of wind evolution and lidar trajectory optimization for lidar-assisted wind turbine control," *Meteorologische Zeitschrift*, 2015. [Online]. Available: http://dx.doi.org/10.1127/metz/2015/0634

[18] D. Schlipf and P. W. Cheng, "Flatness-based feedforward control of wind turbines using lidar," in *Proceedings of the 19th World Congress of the International Federation of Automatic Control*, Cape Town, South Africa, 2014.

[19] A. Körber and R. King, "Nonlinear model predictive control for wind turbines," in *Proceedings of the European Wind Energy Association annual event*, Brussels, Belgium, 2011.

[20] S. Gros, "An economic NMPC formulation for wind turbine control," in *Proceedings of the Conference on Decision and Control*, Florence, Italy, 2013.